

“Super p53” Mice Display Retinal Astroglial Changes

Juan J. Salazar^{1,2}, Roberto Gallego-Pinazo^{5,6}, Rosa de Hoz^{1,2}, Maria D. Pinazo-Durán⁶, Blanca Rojas^{1,3}, Ana I. Ramírez^{1,2}, Manuel Serrano⁴, José M. Ramírez^{1,3*}

1 Instituto de Investigaciones Oftalmológicas “Ramón Castroviejo”, Universidad Complutense de Madrid, Madrid, Spain, **2** Facultad de Óptica y Optometría, Universidad Complutense de Madrid, Madrid, Spain, **3** Facultad de Medicina, Universidad Complutense de Madrid, Madrid, Spain, **4** Spanish National Cancer Research Center, Madrid, Spain, **5** Ophthalmology Department of the University and Polytechnic Hospital La Fe, Valencia, Spain, **6** Ophthalmic Research Unit “Santiago Grisolia” Faculty of Medicine, University of Valencia, Valencia, Spain

Abstract

Tumour-suppressor genes, such as the p53 gene, produce proteins that inhibit cell division under adverse conditions, as in the case of DNA damage, radiation, hypoxia, or oxidative stress (OS). The p53 gene can arrest proliferation and trigger death by apoptosis subsequent to several factors. In astrocytes, p53 promotes cell-cycle arrest and is involved in oxidative stress-mediated astrocyte cell death. Increasingly, astrocytic p53 is proving fundamental in orchestrating neurodegenerative disease pathogenesis. In terms of ocular disease, p53 may play a role in hypoxia due to ischaemia and may be involved in the retinal response to oxidative stress (OS). We studied the influence of the p53 gene in the structural and quantitative characteristics of astrocytes in the retina. Adult mice of the C57BL/6 strain (12 months old) were distributed into two groups: 1) mice with two extra copies of p53 (“super p53”; n = 6) and 2) wild-type p53 age-matched control, as the control group (WT; n = 6). Retinas from each group were immunohistochemically processed to locate the glial fibrillary acidic protein (GFAP). GFAP+ astrocytes were manually counted and the mean area occupied for one astrocyte was quantified. Retinal-astrocyte distribution followed established patterns; however, morphological changes were seen through the retinas in relation to p53 availability. The mean GFAP+ area occupied by one astrocyte in “super p53” eyes was significantly higher ($p < 0.05$; Student’s t-test) than in the WT. In addition, astroglial density was significantly higher in the “super p53” retinas than in the WT ones, both in the whole-retina ($p < 0.01$ Student’s t-test) and in the intermediate and peripheral concentric areas of the retina ($p < 0.05$ Student’s t-test). This fact might improve the resistance of the retinal cells against OS and its downstream signalling pathways.

Citation: Salazar JJ, Gallego-Pinazo R, de Hoz R, Pinazo-Durán MD, Rojas B, et al. (2013) “Super p53” Mice Display Retinal Astroglial Changes. PLoS ONE 8(6): e65446. doi:10.1371/journal.pone.0065446

Editor: Steven Barnes, Dalhousie University, Canada

Received: January 7, 2013; **Accepted:** April 24, 2013; **Published:** June 7, 2013

Copyright: © 2013 Salazar et al. This is an open-access article distributed under the terms of the Creative Commons Attribution License, which permits unrestricted use, distribution, and reproduction in any medium, provided the original author and source are credited.

Funding: Work at the Institute of Ophthalmic Research “Ramón Castroviejo” (Madrid) has been funded by RETICs Patología Ocular del Envejecimiento, Calidad Visual y Calidad de Vida (Grant ISCIII RD07/0062/0000, Spanish Ministry of Science and Innovation); RETICs Prevención, detección precoz y tratamiento de la patología ocular prevalente degenerativa y crónica (Grant ISCIII RD12/0034/0002, Spanish Ministry of Science and Innovation); BSCH-UCM (GR35/10-A Programa de Grupos de Investigación Santander-UCM); BIG is currently supported by a predoctoral fellowship from the Universidad Complutense de Madrid. Work at the Ophthalmic Research Unit “Santiago Grisolia” (Valencia) has been funded by RETICs Prevención, detección precoz y tratamiento de la patología ocular prevalente degenerativa y crónica (Grant ISCIII RD12/0034/0008, Spanish Ministry of Science and Innovation). The funders had no role in study design, data collection and analysis, decision to publish, or preparation of the manuscript.

Competing Interests: The authors have declared that no competing interests exist.

* E-mail: ramirez@med.ucm.es

Introduction

The p53 tumour-suppressor gene is expressed ubiquitously in all cell types as an inactive, latent transcription factor that becomes active only when the cells are subjected to a variety of cellular insults such as DNA damage, radiation, hypoxia, telomere erosion, nutrient deprivation, transcription inhibition, depletion of nucleotide pools, oncogene expression, heat shock, or oxidative stress (OS), among others [1–6]. The activation of p53 triggers a complex transcriptional program that, depending on the cell type, environment, and other contributing factors, induces a number of different responses, ranging from the induction of cell-cycle arrest, programmed cell death, and senescence, to DNA repair, control of mitochondrial respiration, and angiogenesis inhibition [7–9].

Recently, an evolving concept in cell and molecular neuroscience is that glial cells are far more fundamental to disease progression than previously thought, possibly through a noncell-autonomous mechanism that is heavily dependent on p53 activities [10]. In astrocytes, p53 promotes cell-cycle arrest by repressing c-

myc transcription and/or by activating the cyclin-dependent kinase inhibitor p21cip/Cdkn1a [11–14]. Increasingly, astrocytic p53 is proving fundamental in orchestrating neurodegenerative disease pathogenesis. It has been reported that NMDA-mediated CNS excitotoxicity generates a hypertrophic astrocyte morphology associated with changes in p53 expression and nuclear active caspase-3 in the absence of cell death [15]. In addition, p53 is involved in oxidative stress-mediated astrocyte death after stimulation by the intercellular messenger nitric oxide (NO) [16] and by direct, transcription-independent signalling to the mitochondria [17].

Under normal physiological conditions, p53 may help to lower intracellular reactive oxidative species (ROS) levels by promoting glutathione-dependent ROS scavenging [18,19]. In terms of ocular disease, p53 may play a role in hypoxia due to ischaemia [20], leads to G1 arrest upon retinal exposure to ionizing radiation [21–23], and is involved in the retinal response to OS, since p53 can stimulate the expression of specific genes that minimize or block OS [18,19,24–26].

The retina is particularly sensitive to OS because of its oxygen- and lipid-rich environment [27–29]. The OS and its downstream signalling pathways have been related to the pathogenesis of potentially blinding ocular diseases, including glaucoma, diabetic retinopathy and age-related macular degeneration (ARMD) [30–34]. There is substantial evidence that astrocytes have key functions in antioxidant processes [35] because they possess high concentrations of antioxidant enzymes (vitamin E, ascorbate, glutathione). This constitutive expression of antioxidants indicates that astrocytes may take part in the early detoxification of ROS, before inducible scavengers are synthesised [36].

Garcia-Cao et al. (2002) generated “super p53” mice carrying supernumerary fully functional copies of the p53 gene in the form of large genomic transgenes. These super p53 mice were significantly protected from cancer when compared with normal mice and showed no indication of premature ageing. This latter finding is the result of the normal regulation of the supernumerary p53 gene. Because of this, basal levels of p53 activity remained unaltered [37].

In the present study, we take advantage of this experimental model to further challenge the role of p53 in retinal macroglia. For this, we study qualitative and quantitative changes in the astrocyte populations of the super p53 mice retinas, as compared to the WT ones.

Materials and Methods

1. Ethics Statement

Mice were treated in accordance with the Spanish Laws and the Guidelines for Humane Endpoints for Animals Used in Biomedical Research. The Spanish National Cancer Research Centre (CNIO) is part of the “Carlos III” Health Institute (ISCIII) and all protocols were previously submitted to and approved by the Ethics Committee of the ISCIII; approval ID numbers: PA-45 v2, PA-312, and PA-130/07. Also, animal manipulations followed institutional guidelines, European Union regulations for the use of animals in research, and the ARVO (Association for Research in Vision and Ophthalmology) statement for the use of animals in ophthalmic and vision research.

2. Animals and Anaesthetics

Two groups of mice of the C57BL/6 strain, aged 12 months, were considered: i) genetically manipulated mice by introducing two extra copies of p53 gene [37] (“super p53”; $n = 6$) and ii) wild-type age-matched control (WT; $n = 6$). The generation and genotyping of transgenic mice has been previously described [37]. All animals were housed in cages, maintained in temperature- and light-controlled rooms with a 12-h light/dark cycle. Animals had *ad libitum* access to food and water. Light intensity within the cages ranged from 9 to 24 luxes. Mice were maintained under constant conditions for at least 7 days prior to the experiments, which were conducted in the tumour-suppression laboratory (National Oncology Research Centre, Madrid, Spain).

Animals from both groups were examined for morphological characteristics and weighed, and all data were recorded. The mice were deeply anesthetized with an intraperitoneal (i.p.) injection of a mixture of Ketamine (75 mg/kg, Ketolar®, Parke-Davies, S.L., Barcelona, Spain) and Xylazine (10 mg/kg, Rompún®, Bayer, S.A., Barcelona, Spain) and were perfused transcardially through the ascending aorta first with saline and then with 4% paraformaldehyde in 0.1 M phosphate buffer (PB) (pH 7.4). The eyes were post-fixed for 4 h in the same fixative (4% paraformaldehyde in 0.1 M PB at pH 7.4) and kept in sterile 0.1 M PB. The

retinas from both groups were dissected and processed as retinal whole-mounts and used for immunohistochemical techniques [38].

3. Immunohistochemistry

3.1. Staining procedure. The mice retinas were immunostained as described elsewhere [39] with anti-GFAP (GFAP clone GA-5; Sigma, USA) in a 1/150 dilution. Binding sites of the primary antibody were visualized after two days of incubation with the corresponding secondary antibody: the immunoglobulin fraction of goat antimouse antibody conjugated to fluorescein isothiocyanate (FICT) (Sigma, Saint Louis, Missouri, USA) diluted 1/100. A negative control was performed to demonstrate that the secondary antibody reacted only with their respective primary antibody. This control was made by eliminating primary antibody and replacing it with antibody diluent. In addition to identifying the contribution of the endogenous fluorescence to the observed label, a sample of tissue was incubated in all the buffers and detergents used in the experiment but without antibodies.

3.2. Retinal analysis and astrocyte counting. Mice retinal whole-mounts were examined and photographed with a fluorescence microscope (Zeiss, Axioplan 2 Imaging Microscope) equipped with appropriate filter for fluorescence-emission spectra of fluorescein isothiocyanate (Filter set 10, Zeiss).

Retinal astrocytes were quantified following a masked procedure. Quantification was made in the retinal whole-mount as follows. Each entire retinal whole-mount was analysed using the motorized stage of the microscope to scan the whole preparation along the x-y-z axis. Thus, all subsequent fields analysed were contiguous and were examined systematically to ensure that no portion of the retinal whole-mount would be omitted or duplicated. Photographs of these fields were taken at 20 \times , providing an area of 0.18890 mm² and GFAP(+) astrocytes were manually counted in each photograph using the manual counting tool of the Metamorph Imaging System.

For the study of astrocyte distribution each retinal whole mount was divided into three zones that extended concentrically from the optic nerve to the periphery as follows: central (zone 1), intermediate (zone 2), and peripheral (zone 3). Equivalent areas of the retina were consistently selected for each retinal whole-mount, which included zone 1, 2 and 3 (Fig. 1).

To analyse the area occupied for each astrocyte, we used a computer-assisted morphometric analysis system (Metamorph Imaging System, version 5; Universal Imaging Corp., Downingtown, PA, USA) in association with an imaging microscope (Axioplan 2; Zeiss, Göttingen, Germany). Ten to twelve photomicrographs from each animal were taken at random from each retina. The only selection criteria were good tissue quality, good staining, clear visualization of astrocytes, and no GFAP+ Müller cells. Photographs were taken at 20 \times , covering an area of 0.18890 mm². The resulting images were processed first with the detect edges command and then with the auto threshold command of the computer-assisted morphometric analysis system (Metamorph Imaging System, version 5; Universal Imaging Corp.). The “detect edges” command isolates and enhances the edges in an image by using a selected edge-detection convolution which detects edges in the image by comparing brightness changes in the neighbouring pixels. The thresholding command defines a range of gray-scale values found on the pixels of objects of interest, differentiating them from other parts of the image based on the images’ gray scale. Areas of the image that were marked with the red threshold overlay as a visual indicator of the thresholded areas were included in the measurement and processing [40–42]. Thus, in each photograph astrocytes were: i) first, outlined with the detect-edges command and; ii) second, marked with a red

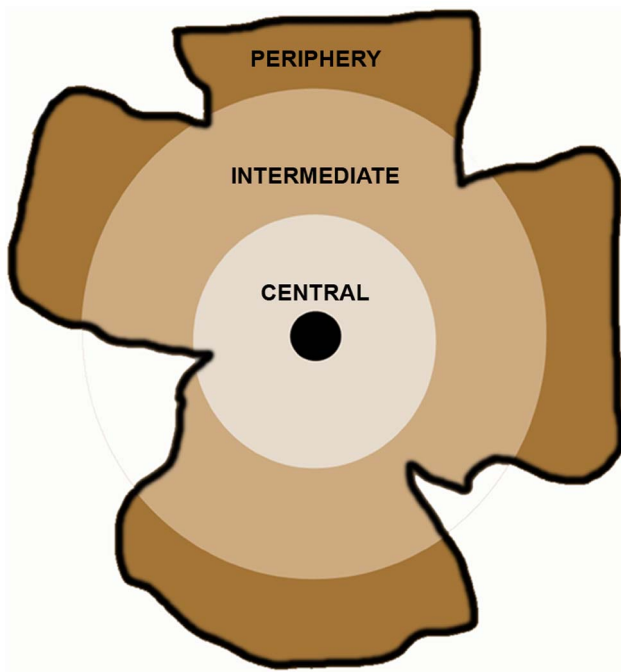


Figure 1. Division of the retina in concentric zones for study.
doi:10.1371/journal.pone.0065446.g001

threshold overlay (as a visual indicator of the threshold areas) for automatic calculation of the area occupied by GFAP+ astrocytes; iii) third, manually counted. To determine the mean GFAP+ area occupied by one astrocyte, the GFAP+ area of each picture was divided by the number of thresholded astrocytes in that picture.

4. Statistical Procedures

The statistical data were entered on a spread sheet (Excel Microsoft Co, Redmond, WA, USA) and descriptive statistics (mean \pm SDM in the figure) were calculated. Differences between groups were evaluated and processed in a SPSS 19.0 (comprehensive statistical software, SPSS sciences Inc©, Chicago, IL, USA). Significance levels were set at $P < 0.05$ (*), $P < 0.01$ (**).

The unpaired Student's t-test was used to compare: i) astrocyte number between WT and “super p53” mice retinas; ii) astrocyte number among the three concentric zones of the retina selected for study (central, intermediate, and peripheral); iii) mean GFAP+ area occupied by one astrocyte between WT and “super p53”.

Results

The mice from the two groups showed no statistically significant changes in the body weight, size, eyes, or ocular adnexa tissues examined.

1. GFAP Staining

1.1. wild-type C57BL/6 mice. In WT retinas, GFAP+ astrocytes were spaced regularly throughout the nerve-fibre retinal ganglion cell (RCG) layer as viewed from the surface, forming a homogeneous plexus (Fig. 2B) evenly distributed throughout the retina from the disc to the periphery. This plexus was composed mainly of stellate-shaped cells (Fig. 3A) that could easily be distinguished from each other (Fig. 2B). These cells had a rounded body from which numerous primary and secondary processes extended (Fig. 3A). Astrocyte processes reached other astrocytes or

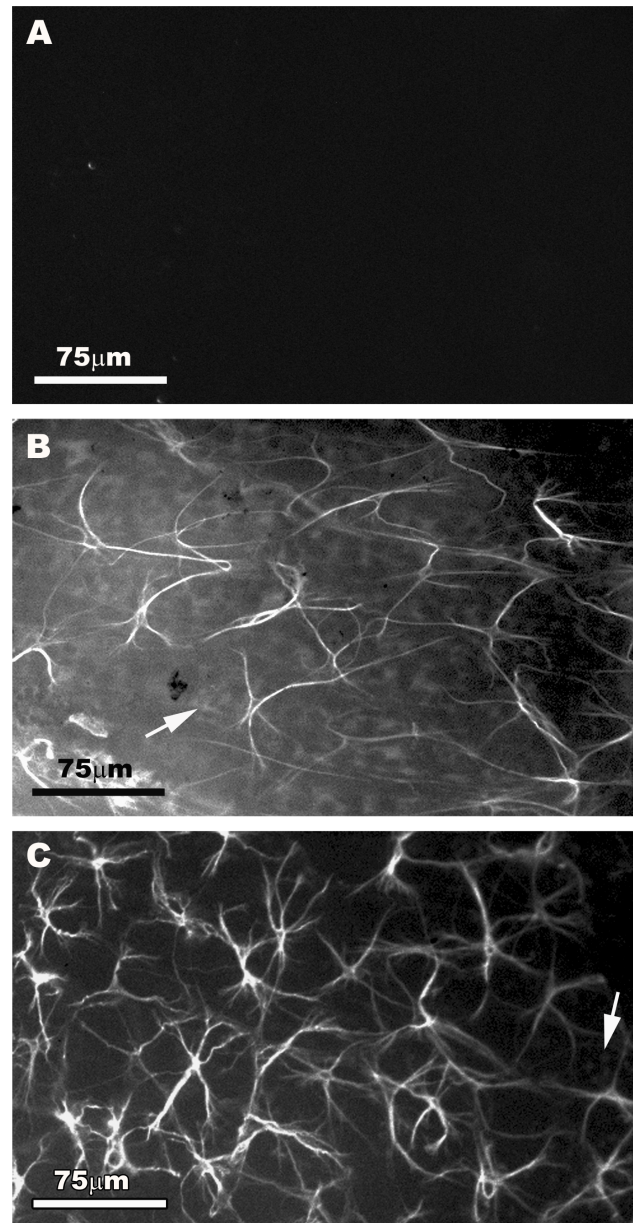


Figure 2. Astroglial plexus of equivalent areas (central zone) of the retinal whole-mounts in WT and “super p53” mice. GFAP immunofluorescence. A: negative control for GFAP immunostaining, B: WT. C: “super p53”. In both B and C, Müller cells appeared as faint GFAP+ punctated structures between astrocytes in some retinal areas (arrow) and astrocytes formed a homogeneous plexus on the nerve-fiber-RCG layer of GFAP+ cells regularly distributed throughout the retina. This plexus was composed of stellate cells that could easily be distinguished from each other. In “super p53” the astrocyte plexus was denser than in WT. [WT: wild type p53 age-matched control; “super p53”: mice with two extra copies of p53].
doi:10.1371/journal.pone.0065446.g002

blood vessels and formed the astroglial plexus (Fig. 2B). Some areas of the retina showed a faint GFAP immunoreactivity (IR) in Müller cells which appeared as punctuate structures between the astrocytes and their radiating processes (Fig. 2B).

1.2. super-p53 mice. Like WT, astrocytes in “super p53” eyes formed a homogeneous plexus of star-shaped cells evenly distributed throughout the retina from the disc to the periphery. At

first sight, the astrocyte plexus in “super p53” eyes appeared to be denser than in WT (Fig. 2). The analysis of the tissues at higher magnification, looking for morphological features that might contribute to this impression, revealed that the soma and primary processes of astrocytes in “super p53” retinas were apparently more robust and the secondary processes were more evident than in WT and spread out like a fan (Fig. 3). We calculated the mean area GFAP+ occupied by one astrocyte in order to ascertain whether this parameter could at least partly explain the subjective impression that in “super p53” retinas the astrocytes were more robust and the astroglial plexus denser than in WT. The analysis of these data revealed that the mean GFAP+ area occupied by one astrocyte in “super p53” eyes was significantly higher ($p < 0.05$; Student's t-test) (Fig. 4) than in the WT.

No differences in GFAP-IR in Müller cells were observed with respect to the WT.

1.3. Astrocyte number. Another feature that could account for the denser appearance of the astrocyte plexus in “super p53” retinas was that the astrocytes were significantly more numerous (3414.80 ± 258.00) than in the WT (1933.00 ± 522.21) ($p < 0.01$; Student's t-test) (Fig. 5). In the analysis made by concentric zones, “super p53” animals had significantly more astrocytes than WT in the intermediate (70.76 ± 10.69 vs. 53.38 ± 8.51 , respectively) and peripheral zones (71.11 ± 12.11 vs. 41.19 ± 12.91 , respectively) ($p < 0.05$, Student's t-test in both instances).

Discussion

Much of the early data reported on p53 were gathered using techniques that, in general, lack cell resolution, such as PCR, Western blot, and ELISA. Moreover, many of the initial studies linking p53 with nervous-system injury and degeneration somewhat overlooked the involvement of glia, and thus arrived at neuron-centred conclusions [10,43–49]. To the best of our knowledge, this is the first study available to show the morphological features, distribution, and number of retinal astrocytes in “super p53” mice retina.

In the “super p53” mice retina, the supernumerary p53 gene was closely related to a significantly increased population of retinal astroglia when the quantification included the whole retina. This significant increase in astrocyte number was also detected in the intermediate and peripheral zones of the retina. In “super p53” the central zone, there was an area, near the optic-nerve margins, where the large amount of astrocytes made it difficult to discern cells individually, thus precluding quantification. This could be the reason why no significant differences in astrocyte number in the central zone were found between the two study groups.

The significant increase in the mean GFAP+ area occupied by one astrocyte in “super p53” eyes in comparison with WT, could explain our subjective impression that, in “super p53” mice retina, astrocytes were more robust and formed a denser astroglial network than in the WT mice. These features are exhibited by reactive astrocytes [50–53]. Studies of neurological disorders indicate that reactive gliosis may have either a positive or negative effect on neuronal function and maintenance [52]. The task of reactive astrocytes is assumed to be that of protecting the neurons by producing neurotrophic factors, increasing the expression of antioxidant enzymes, augmenting the transport and production of glucose [54,55], regulating the removal of harmful substances produced by damaged neurons and promoting neuronal growth [56,57], among others. Notably, these reactive gliosis-like changes of astrocytes in “super p53” retinas did not run in parallel with an increment in GFAP-immunoreactivity (IR) in Müller cells. By contrast, Ueki et al [58] analysed GFAP expression in retinal

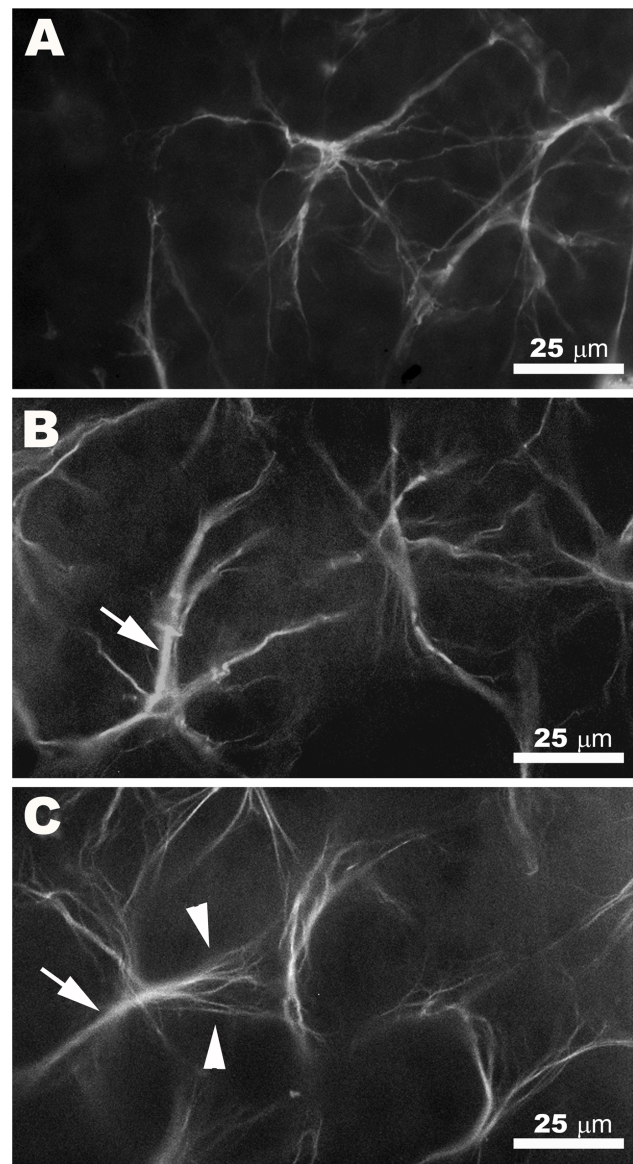


Figure 3. Morphological features of retinal astrocytes in WT and “super p53” mice. GFAP immunofluorescence. A: WT. B–C: “super p53”. In WT and “super p53” eyes, astrocytes had a rounded body from which numerous primary and secondary processes extended. In “super p53” eyes the soma and the primary processes (arrow) had a more robust appearance than in WT. Secondary processes of astrocytes in “super p53” were more evident than WT and spread out like a fan (arrowhead). [WT: wild type p53 age-matched control; “super p53”: mice with two extra copies of p53]. doi:10.1371/journal.pone.0065446.g003

Müller cells in mouse *Trp53*^{−/−} and found greater expression of this marker of reactive gliosis.

It has been proposed that an increase in p53 functionality, while beneficial to prevent tumour development, can be detrimental to long-term viability because it may accelerate the ageing process [59]. In human [60,61] and rat [62,63] retina, ageing is associated with a progressive decline in astrocyte number. The significant increase in the number of retinal astrocytes in the “super p53” group reinforces the idea that these mice lack signs of premature ageing. This may be related to the normal regulation of the supernumerary p53 animals [37].

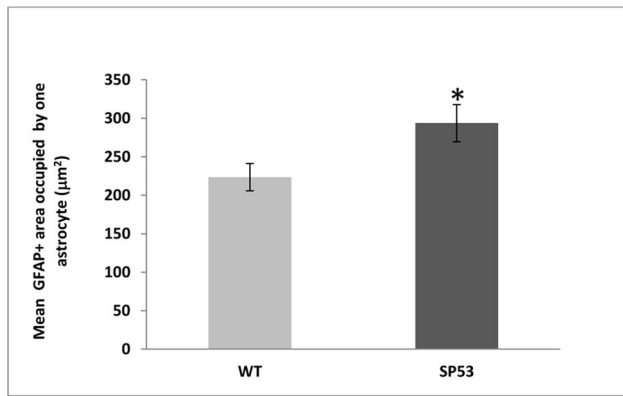


Figure 4. Mean GFAP+ area occupied by one astrocyte. In “super p53” retinas the mean GFAP+ area occupied by one astrocyte was significantly higher ($*P<0.05$; Student’s t-test) than in WT retinas. Columns represent mean \pm SDM of GFAP+ area. [WT: wild type p53 age-matched control; “super p53”: mice with two extra copies of p53]. doi:10.1371/journal.pone.0065446.g004

The “super p53” retinas showed more astrocytes, which also had more evident secondary processes to interact with neighbouring neuronal cells. This could be a factor to increase the neuro-supporting role of astrocytes. In the human retina, astroglial processes join together by means of desmosomes [64,65] and gap junctions [65] to form a mesh that reinforces the capillary network and supports the neurons present in the glial network. These kinds of junctions between processes have also been reported in rats [66] as well in other animal species [67,68]. It is known that astrocytes play a decisive role in the metabolism of neurotransmitters and CO₂. Moreover, ions, most sugars, amino acids, nucleotides, vitamins, hormones, and cyclic AMC pass through gap junctions. Apart from coordinating the metabolic activity of cell populations, gap junctions may also participate in electrical activities or amplify the consequences of signal transduction [69]. Recently another kind of cell-cell communication, i.e. tunneling-nanotubes (TNTs), has been described [70]. TNTs are thin membranous extensions that form channels between cells for intercellular communication and trafficking and are found in numerous cell types, including neurons and astrocytes [71,72]. The p53 gene is involved in TNT development. Cell insults activate p53 and induce M-Sec overexpression, which can trigger F-actin polymerization and contribute to TNT development from the initiating cell membrane [73,74]. The apparent increment of astrocyte secondary processes found in this study could mean an increase of their gap junctions and TNTs and, consequently, an improvement in cell-cell interactions and neural function.

There is clear evidence for a role of p53 in the regulation of oxidative stress [75]. Although the apoptotic activity of p53 is mediated, at least partly, by rising ROS levels [76,77], a number of studies have shown a survival function for p53 in lowering intracellular ROS levels, involving the activity of p53-inducible genes such as TIGAR, sestrins [78,79], aldehyde dehydrogenase-4 (ALDH4) [80], and others [81]. Most notably, this antioxidant

References

- Ljungman M (2000) Dial 9-1-1 for p53: Mechanisms of p53 activation by cellular stress. *Neoplasia* 2: 208–225.
- Pluquet O, Hainaut P (2001) Genotoxic and non-genotoxic pathways of p53 induction. *Cancer Lett* 174: 1–15.
- Llanos S, Efeyan A, Monsech J, Dominguez O, Serrano M (2006) A high-throughput loss-of-function screening identifies novel p53 regulators. *Cell Cycle* 5: 1880–1885.

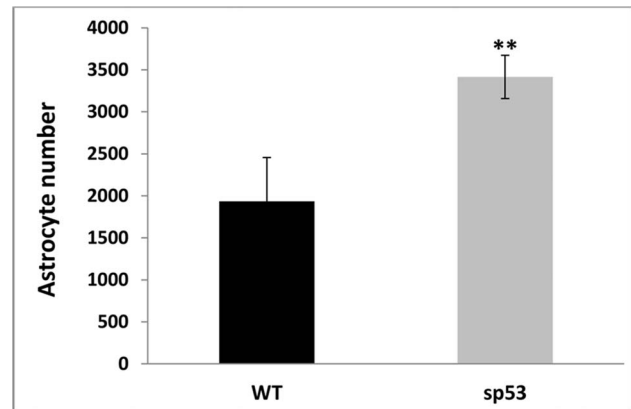


Figure 5. Astrocyte quantification in the entire retinal whole-mount. Total number of astrocytes in “super p53” retinas were significantly more numerous than in WT retinas ($**p<0.01$; Student’s t-test). Columns represent the mean number \pm SDM of GFAP+ astrocytes [WT: wild type p53 age-matched control; “super p53”: mice with two extra copies of p53]. doi:10.1371/journal.pone.0065446.g005

function of p53 is important in the absence of acute stress, preventing the accumulation of DNA damage on a day-to-day basis [24]. An increased p53 gene dosage confers the retina with noticeable resistance to OS, presumably by boosting antioxidant activity and opening anti-apoptotic pathways [82]. We have recently reported an increase in the total antioxidant activity in the optic nerve and retina of “super p53” with respect to WT animals [83,84]. This higher antioxidant activity could indicate that p53 may modulate OS-derived retinal damage. The higher number of astrocytes found in the retinas of “super p53” mice in the present work could be responsible for the augmented antioxidant capacity observed [83,84].

The most noteworthy finding of this study is the significant increase in the retinal astrocyte population of “super p53” mice. This increase might improve the resistance of the retinal cells against ROS and its downstream signalling pathways. These findings could be the starting point to develop future treatments for those diseases such as diabetic retinopathy, glaucoma, or ARMD, the pathogenesis of which involves oxidative stress.

Acknowledgments

We thank Desirée Contreras, Francisca Vargas for technical assistance, Maribel Muñoz for great animal assistance and David Nesbitt for correcting the English version of this work.

Author Contributions

Conceived and designed the experiments: MS RGP MDPD JMR. Performed the experiments: JJS RdH BR AIR MS RGP MDPD JMR. Analyzed the data: JJS RdH BR AIR JMR. Contributed reagents/materials/analysis tools: JJS RdH BR AIR MS RGP MDPD JMR. Wrote the paper: JJS RdH BR AIR JMR.

- Vousden KH, Lane DP (2007) p53 in health and disease. *Nat Rev Mol Cell Bio* 8: 275–283.
- Levine AJ, Oren M (2009) The first 30 years of p53: Growing ever more complex. *Nat Rev Cancer* 9: 749–758.
- Villasante A, Piazzolla D, Li H, Gómez-López G, Djabali M, et al. (2011) Epigenetic regulation of nanog expression by Ezh2 in pluripotent stem cells. *Cell Cycle* 10: 1488–1498.

7. Collado M, Serrano M (2005) The senescent side of tumor suppression. *Cell Cycle* 4: 1722–1724.
8. Riley T, Sontag E, Chen P, Levine A (2008) Transcriptional control of human p53-regulated genes. *Nat Rev Mol Cell Bio* 9: 402–412.
9. Suzuki K, Matsubara H (2011) Recent advances in p53 research and cancer treatment. *J Biomed Biotechnol* 2011: ID 978312.
10. Jebelli JD, Hooper C, Garden GA, Pocock JM (2012) Emerging roles of p53 in glial cell function in health and disease. *Glia* 60: 515–525.
11. Cox LS, Lane DP (1995) Tumour suppressors, kinases and clamps: How p53 regulates the cell cycle in response to DNA damage. *Bioessays* 17: 501–508.
12. Kippin TE, Martens DJ, Van Der Kooy D (2005) p21 loss compromises the relative quiescence of forebrain stem cell proliferation leading to exhaustion of their proliferation capacity. *Gene Dev* 19: 756–767.
13. Meletis K, Wirta V, Hede SM, Nistér M, Lundeberg J, et al. (2006) p53 suppresses the self-renewal of adult neural stem cells. *Development* 133: 363–369.
14. Zheng H, Ying H, Yan H, Kimmelman AC, Hiller DJ, et al. (2008) p53 and pten control neural and glioma stem/progenitor cell renewal and differentiation. *Nature* 455: 1129–1133.
15. Villapol S, Acarin L, Faiz M, Castellano B, Gonzalez B (2007) Distinct spatial and temporal activation of caspase pathways in neurons and glial cells after excitotoxic damage to the immature rat brain. *J Neurosci Res* 85: 3545–3556.
16. Yung HW, Bal-Price AK, Brown GC, Tolkovsky AM (2004) Nitric oxide-induced cell death of cerebrocortical murine astrocytes is mediated through p53- and Bax-dependent pathways. *J Neurochem* 89: 812–821.
17. Bonini P, Cicconi S, Cardinale A, Vitale C, Serafino AL, et al. (2003) Oxidative stress induces p53-mediated apoptosis in glia: P53 transcription-independent way to die. *J Neurosci Res* 75: 83–95.
18. Matheu A, Maraver A, Klatt P, Flores I, Garcia-Cao I, et al. (2007) Delayed ageing through damage protection by the Arf/p53 pathway. *Nature* 448: 375–379.
19. Bensaad K, Tsuruta A, Selak MA, Vidal MN, Nakano K, et al. (2006) TIGAR, a p53-inducible regulator of glycolysis and apoptosis. *Cell* 126: 107–120.
20. Joo CK, Choi JS, Ko HW, Park K, Sohn S, et al. (1999) Necrosis and apoptosis after retinal ischemia: Involvement of NMDA-mediated excitotoxicity and p53. *Invest Ophthalmol Vis Sci* 40: 713–720.
21. Morgan SE, Kastan MB (1997) Foundations in cancer research p53 and ATM: Cell cycle, cell death, and cancer. *Adv Cancer Res* 71: 1–25.
22. Borges H, Chao C, Xu Y, Linden R, Wang J (2004) Radiation-induced apoptosis in developing mouse retina exhibits dose-dependent requirement for ATM phosphorylation of p53. *Cell Death Differ* 11: 494–502.
23. Miller TJ, Schneider RJ, Miller JA, Martin BP, Al-Ubaidi MR, et al. (2006) Photoreceptor cell apoptosis induced by the 2-nitroimidazole radiosensitizer, CI-1010, is mediated by p53-linked activation of caspase-3. *Neurotoxicology* 27: 44–59.
24. Sablina AA, Budanov AV, Ilyinskaya GV, Agapova LS, Kravchenko JE, et al. (2005) The antioxidant function of the p53 tumor suppressor. *Nat Med* 11: 1306–1313.
25. Matoba S, Kang JG, Patino WD, Wragg A, Boehm M, et al. (2006) P53 regulates mitochondrial respiration. *Science* 312: 1650–1653.
26. O'Connor JC, Wallace DM, O'Brien CJ, Cotter TG (2008) A novel antioxidant function for the tumor-suppressor gene p53 in the retinal ganglion cell. *Invest Ophthalmol Vis Sci* 49: 4237–4244.
27. Wiegand R, Giusto NM, Rapp LM, Anderson RE (1983) Evidence for rod outer segment lipid peroxidation following constant illumination of the rat retina. *Invest Ophthalmol Vis Sci* 24: 1433–1435.
28. Organisciak DT, Vaughan DK (2010) Retinal light damage: Mechanisms and protection. *Prog Ret Eye Res* 29: 113–134.
29. Beatty S, Koh H, Phil M, Henson D, Boulton M (2000) The role of oxidative stress in the pathogenesis of age-related macular degeneration. *Surv Ophthalmol* 45: 115.
30. Lipton SA (2001) Retinal ganglion cells, glaucoma and neuroprotection. *Prog Brain Res* 131: 712–718.
31. Ohia SE, Opere CA, Leday AM (2005) Pharmacological consequences of oxidative stress in ocular tissues. *Mut Res* 579: 22–36.
32. Zanon-Moreno V, Marco-Ventura P, Lleo-Perez A, Pons-Vazquez S, Garcia-Medina JJ, et al. (2008) Oxidative stress in primary open-angle glaucoma. *J Glaucoma* 17: 263–268.
33. Harada C, Namekata K, Guo X, Yoshida H, Mitamura Y, et al. (2010) ASK1 deficiency attenuates neural cell death in GLAST-deficient mice, a model of normal tension glaucoma. *Cell Death Differ* 17: 1751–1759.
34. Mancino R, Di Pierro D, Varesi C, Cerulli A, Feraco A, et al. (2011) Lipid peroxidation and total antioxidant capacity in vitreous, aqueous humor, and blood samples from patients with diabetic retinopathy. *Mol Vis* 17: 1298.
35. Hirrlinger PG, Ulbricht E, Iandiev I, Reichenbach A, Pannicke T (2010) Alterations in protein expression and membrane properties during muller cell gliosis in a murine model of transient retinal ischemia. *Neurosci Lett* 472: 73–78.
36. Dirnagl U, Priller J, Dirnagl U, Priller J (2004) Focal cerebral ischemia: The multifaceted role of glial cells. *Neuroglia*. New York: Oxford.p 520.
37. Garcia-Cao I, Garcia-Cao M, Martin-Caballero J, Criado LM, Klatt P, et al. (2002) “Super p53” mice exhibit enhanced DNA damage response, are tumor resistant and age normally. *EMBO J* 21: 6225–6235.
38. Ramirez JM, Triviño A, Ramirez AI, Salazar JJ, Garcia-Sánchez J (1994) Immunohistochemical study of human retinal astroglia. *Vision Res* 34: 1935–1946.
39. Triviño A, Ramirez JM, Ramirez AI, Salazar JJ, Garcia-Sánchez J (1992) Retinal perivascular astroglia: An immunoperoxidase study. *Vision Res* 32: 1601–1607.
40. Ramirez AI, Salazar JJ, de Hoz R, Rojas B, Ruiz E, et al. (2006) Macroglial and retinal changes in hypercholesterolemic rabbits after normalization of cholesterol levels. *Exp Eye Res* 83: 1423–1438.
41. Ramirez AI, Salazar JJ, de Hoz R, Rojas B, Gallego BI, et al. (2010) Quantification of the effect of different levels of IOP in the astroglia of the rat retina ipsilateral and contralateral to experimental glaucoma. *Invest Ophthalmol Vis Sci* 51: 5690–5696.
42. Gallego BI, Salazar JJ, de Hoz R, Rojas B, Ramirez AI, et al. (2012) IOP induces upregulation of GFAP and MHC-II and microglia reactivity in mice retina contralateral to experimental glaucoma. *J Neuroinflamm* 9: 92.
43. Djebaili M, Rondouin G, Baille V, Bockeaert J (2000) p53 and bax implication in NMDA induced-apoptosis in mouse hippocampus. *Neuroreport* 11: 2973–2976.
44. Martin LJ, Liu Z (2002) Injury-induced spinal motor neuron apoptosis is preceded by DNA single-strand breaks and is p53- and Bax-dependent. *J Neurobiol* 50: 181–197.
45. Morrison RS, Wenzel HJ, Kinoshita Y, Robbins CA, Donchower LA, et al. (1996) Loss of the p53 tumor suppressor gene protects neurons from kainate-induced cell death. *J Neurosci* 16: 1337–1345.
46. Napieralski JA, Raghupathi R, McIntosh TK (1999) The tumor-suppressor gene, p53, is induced in injured brain regions following experimental traumatic brain injury. *Mol Brain Res* 71: 78–86.
47. Qin ZH, Chen RW, Wang Y, Nakai M, Chuang DM, et al. (1999) Nuclear factor κB nuclear translocation upregulates c-myc and p53 expression during NMDA receptor-mediated apoptosis in rat striatum. *J Neurosci* 19: 4023–4033.
48. Sakhi S, Bruce A, Sun N, Tocco G, Baudry M, et al. (1994) p53 induction is associated with neuronal damage in the central nervous system. *PNAS* 91: 7525–7529.
49. Watanabe H, Ohta S, Kumon Y, Sakaki S, Sakanaka M (1999) Increase in p53 protein expression following cortical infarction in the spontaneously hypertensive rat. *Brain Res* 837: 38–45.
50. Malhotra S, Shnitka T, Elbrink J (1990) Reactive astrocytes—a review. *Cytobios* 61: 133.
51. Ridet J, Privat A (2000) Reactive astrocytes, their roles in CNS injury, and repair mechanisms. *Adv Struct Biol* 6: 147–185.
52. Pekny M, Nilsson M (2005) Astrocyte activation and reactive gliosis. *Glia* 50: 427–434.
53. Malhotra A, Minja FJ, Crum A, Burrows D (2011) Ocular anatomy and cross-sectional imaging of the eye. *Semin Ultrasound CT* 32: 2–13.
54. Sofroniew M, Vinters H (2010) Astrocytes: Biology and pathology. *Acta Neuropathol* 119: 7–35.
55. Allaman I, Bélanger M, Magistretti PJ (2011) Astrocyte–neuron metabolic relationships: For better and for worse. *Trends Neurosci* 34: 76–87.
56. Tacconi MT (1998) Neuronal death: Is there a role for astrocytes? *Neurochem Res* 23: 759–765.
57. Carson MJ, Cameron Thrash J, Walter B (2006) The cellular response in neuroinflammation: The role of leukocytes, microglia and astrocytes in neuronal death and survival. *Clin Neurosci Res* 6: 237–245.
58. Ueki Y, Karl MO, Sudar S, Pollak J, Taylor RJ, et al. (2012) P53 is required for the developmental restriction in müller glial proliferation in mouse retina. *Glia* 60: 1579–1589.
59. Tyner SD, Venkatchalam S, Choi J, Jones S, Ghebranious N, et al. (2002) p53 mutant mice that display early ageing-associated phenotypes. *Nature* 415: 45–53.
60. Madigan MC, Penfold PL, Provis JM, Balind TK, Billson FA (1994) Intermediate filament expression in human retinal macroglia. histopathologic changes associated with age-related macular degeneration. *Retina* 14: 65–74.
61. Ramirez JM, Ramirez AI, Salazar JJ, de Hoz R, Triviño A (2001) Changes of astrocytes in retinal ageing and age-related macular degeneration. *Exp Eye Res* 73: 601–615.
62. Cavallotti C, Cavallotti D, Pescosolido N, Pacella E (2003) Age-related changes in rat optic nerve: Morphological studies. *Anat Histol Embryol* 32: 12–16.
63. Mansour H, Chamberlain CG, Weible MW 2nd, Hughes S, Chu Y, et al. (2008) Aging-related changes in astrocytes in the rat retina: Imbalance between cell proliferation and cell death reduces astrocyte availability. *Aging Cell* 7: 526–540.
64. Iku H, Uga S, Kohno T (1976) Electron microscope study on astrocytes in the human retina using ruthenium red. *Ophthalmic Res* 8: 100–110.
65. Ramirez JM, Triviño A, Ramirez AI, Salazar JJ, Garcia-Sánchez J (1996) Structural specializations of human retinal glial cells. *Vision Res* 36: 2029–2036.
66. Zahs KR, Newman EA (1997) Asymmetric gap junctional coupling between glial cells in the rat retina. *Glia* 20: 10–22.
67. Bussow H (1980) The astrocytes in the retina and optic nerve head of mammals: A special glia for the ganglion cell axons. *Cell Tissue Res* 206: 367–378.
68. Hollander H, Makarov F, Dreher Z, van Driel D, Chan-Ling TL, et al. (1991) Structure of the macroglia of the retina: Sharing and division of labour between astrocytes and muller cells. *J Comp Neurol* 313: 587–603.
69. Ramson BR, Ye Z (2005) Gap junctions and hemichannels. In: Ketteman H, Ramson BR, editors. *Neuroglia*. Ney York: Oxford University Press. 177–189.

70. Gerdes HH, Bukoreshtliev NV, Barroso JFV (2007) Tunneling nanotubes: A new route for the exchange of components between animal cells. *FEBS Lett* 581: 2194–2201.
71. Davis DM, Sowinski S (2008) Membrane nanotubes: Dynamic long-distance connections between animal cells. *Nat Rev Mol Cell Biol* 9: 431–436.
72. Zhang Y (2011) Tunneling-nanotube: A new way of cell-cell communication. *CIB* 4: 324–325.
73. Wang M, Ma W, Zhao L, Fariss RN, Wong WT (2011) Adaptive muller cell responses to microglial activation mediate neuroprotection and coordinate inflammation in the retina. *J Neuroinflamm* 8: 173.
74. Hase K, Kimura S, Takatsu H, Ohmae M, Kawano S, et al. (2009) M-sec promotes membrane nanotube formation by interacting with ral and the exocyst complex. *Nat Cell Biol* 11: 1427–1432.
75. Bensaad K, Vouden KH (2005) Savior and slayer: The two faces of p53. *Nat Med* 11: 1278–1279.
76. Johnson TM, Yu ZX, Ferrans VJ, Lowenstein RA, Finkel T (1996) Reactive oxygen species are downstream mediators of p53-dependent apoptosis. *PNAS* 93: 11848–11852.
77. Polyak K, Xia Y, Zweier JL, Kinzler KW, Vogelstein B (1997) A model for p53-induced apoptosis. *Nature* 389: 300–304.
78. Velasco-Miguel S, Buckbinder L, Jean P, Gelbert L, Talbott R, et al. (1999) PA26, a novel target of the p53 tumor suppressor and member of the GADD family of DNA damage and growth arrest inducible genes. *Oncogene* 18: 127.
79. Budanov AV, Sablina AA, Feinstein E, Koonin EV, Chumakov PM (2004) Regeneration of peroxiredoxins by p53-regulated sestrins, homologs of bacterial AhpD. *Sci Signal* 304: 596.
80. Yoon KA, Nakamura Y, Arakawa H (2004) Identification of ALDH4 as a p53-inducible gene and its protective role in cellular stresses. *J Hum Genet* 49: 134–140.
81. Gu S, Liu Z, Pan S, Jiang Z, Lu H, et al. (2004) Global investigation of p53-induced apoptosis through quantitative proteomic profiling using comparative amino acid-coded tagging. *Mol Cell Proteomics* 3: 998–1008.
82. Wasylyk C, Wasylyk B (2000) Defect in the p53-Mdm2 autoregulatory loop resulting from inactivation of TAFII250 in cell cycle mutant tsBN462 cells. *Mol Cell Biol* 20: 5554–5570.
83. Gallego-Pinazo R, Zanón-Moreno V, Sanz S, Andrés V, Serrano M, et al. (2008) Caracterización bioquímica del nervio óptico en el ratón que sobreexpresa el gen p53: Análisis de estrés oxidativo. *Arch Soc Esp Oftalmol* 83: 105–112.
84. Pinazo-Duran MD, Gallego-Pinazo R, Vinuesa Silva I, Zanon-Moreno V, Garcia-Medina JJ, et al. (2007) Biochemical determination of oxidative and antioxidant activities in the retina-choroid of the super P53 mice. *ARVO Meeting Abstracts* 48: 4180.